Angular dependence of the pp elastic scattering spin correlation parameter A_{00nn} between 0.8 and 2.8 GeV: Results for 1.80–2.24 GeV

C. E. Allgower,[1,*] J. Ball,[2,3] L. S. Barabash,[4] P.-Y. Beauvais,[2] M. E. Beddo,[1,†] N. Borisov,[4] A. Boutefnouchet,[5] J. Bystrický,[3] P.-A. Chamouard,[2] M. Combet,[2,3] Ph. Demierre,[6] J.-M. Fontaine,[2,3] V. Ghazikhanian,[5] D. P. Grosnick,[1,‡] R. Hess,[6,§] Z. Janout,[4,∥] Z. F. Janout,[6,¶] V. A. Kalinnikov,[4] T. E. Kasprzyk,[1] Yu. M. Kazarinov,[4,§] B. A. Khachaturov,[4] R. Kunne,[2,**] F. Lehar,[3] A. de Lesquen,[3] D. Lopiano,[1] M. de Mali,[3,§] V. N. Matafonov,[4] I. L. Pisarev,[4] A. A. Popov,[4] A. N. Prokofiev,[7] D. Rapin,[6] J.-L. Sans,[2,††] H. M. Spinka,[1] Yu. A. Usov,[4] V. V. Vikhrov,[7] B. Vuaridel,[6] C. A. Whitten,[5] and A. A. Zhdanov[7]

[1]*Argonne National Laboratory, HEP Division, 9700 South Cass Avenue, Argonne, Illinois 60439*
[2]*Laboratoire National Saturne, CNRS/IN2P3 and CEA/DSM, CEA/Saclay, F-91191 Gif sur Yvette Cedex, France*
[3]*DAPNIA, CEA/Saclay, F-91191 Gif sur Yvette Cedex, France*
[4]*Laboratory of Nuclear Problems, JINR, RU-141980 Dubna, Moscow Region, Russia*
[5]*Physics Department, University of California at Los Angeles, 405 Hilgard Avenue, Los Angeles, California 90024*
[6]*DPNC, University of Geneva, 24 quai Ernest-Ansermet, 1211 Geneva 4, Switzerland*
[7]*Petersburg Nuclear Physics Institute, RU-188350 Gatchina, Russia*

(Received 7 July 2000; published 10 November 2000)

Measurements at 19 beam kinetic energies between 1795 and 2235 MeV are reported for the pp elastic scattering spin correlation parameter $A_{00nn}=A_{NN}=C_{NN}$. The c.m. angular range is typically 60–100°. The measurements were performed at Saturne II with a vertically polarized beam and target (transverse to the beam direction and scattering plane), a magnetic spectrometer and a recoil detector, both instrumented with multiwire proportional chambers, and beam polarimeters. These results are compared to previous data from Saturne II and elsewhere.

PACS number(s): 13.75.Cs, 24.70.+s, 25.10.+s, 25.40.Cm

I. INTRODUCTION

This experiment is part of a systematic study of the nucleon-nucleon system in the Saturne II energy range. Measurements of the spin correlation parameter $A_{00nn}=C_{NN}=A_{NN}=(N,N;0,0)$ for pp elastic scattering (see Ref. [1] for a description of the spin observables) were made at 19 beam kinetic energies between 1.795 and 2.235 GeV and c.m. angles from about 60–100°. The data were obtained with a vertically polarized proton beam incident on a vertically polarized proton target, and the outgoing protons were detected within about $\pm 10°$ of the horizontal plane with scintillation counters and multiwire proportional chambers. The spin correlation parameter is defined as

$$A_{00nn}=\frac{d\sigma/d\Omega(\uparrow\uparrow)+d\sigma/d\Omega(\downarrow\downarrow)-d\sigma/d\Omega(\uparrow\downarrow)-d\sigma/d\Omega(\downarrow\uparrow)}{d\sigma/d\Omega(\uparrow\uparrow)+d\sigma/d\Omega(\downarrow\downarrow)+d\sigma/d\Omega(\uparrow\downarrow)+d\sigma/d\Omega(\downarrow\uparrow)}, \quad (1)$$

where the arrows denote the spin directions of the beam and target, respectively.

The experiment was performed in four run periods spread over a three-year time span. This paper describes data collected in the first two run periods (I, II); results on the analyzing power $A_{00n0}=A_N$ from these same run periods are described in Ref. [2]. Data for A_N from the last two (III, IV) are presented in Ref. [3], and for A_{00nn} will be given in a forthcoming paper. Each run period was 10–14 days in duration, during which measurements were made at a number of energies. Scattering events from the polarized target were collected simultaneously with those from an unpolarized CH_2 target, and these A_N data are published in Ref. [4]. Results on the spin observables K_{0nn0} and D_{0n0n} from these same run periods are given in Ref. [5]. Some of the A_{00nn}

*Present address: Indiana University Cyclotron Facility, Bloomington, IN 47408.

†Present address: Data Ventures LLC, Los Alamos, NM 87544.

‡Present address: Department of Physics and Astronomy, Ball State University, Muncie, IN 47306.

§Deceased.

∥Present address: Faculty of Nuclear Sciences and Physical Engineering, Czech Technical University, Brehová 7, 11519 Prague 1, Czech Republic.

¶Present address: Computing Center of the Czech Technical University, Zikova 4, 16635 Prague 6, Czech Republic.

**Present address: Institut de Physique Nucléaire IN2P3, F-91400 Orsay, France.

††Present address: Centrale Themis, F-66121 Targasonne, France.

0556-2813/2000/62(6)/064001(11)/$15.00

data in this paper were previously reported in Ref. [6]; they have been reanalyzed using improved techniques for this paper.

Many details of the experimental apparatus are given in Refs. [2,3,7–12]. A brief description of the polarized beam and target occurs in Sec. II, and of the detectors for the outgoing protons in Sec. III. A short discussion of the data analysis is presented in Sec. IV, and the results are given in Sec. V.

II. POLARIZED BEAM AND TARGET

The polarized beam was produced in an atomic beam-type polarized ion source and accelerated in both the Mimas booster ring and the Saturne II accelerator. Four different beam polarization states were used at most energies during run period II, designated 0_+ (state 1), – (state 2), + (state 3), and 0_- (state 4); only the + and – states were used during most data collected in run period I. The polarization of the beam pulses normally alternated in the pattern 0_+, –, +, 0_-, –, +, 0_+, –, +, 0_-, $\cdots$ (or +, –, +, –, + $\cdots$ for run period I). The relative direction is given by the + and – signs in the designation of these four vertically polarized states. Certain beam energy ranges had + corresponding to vertically up, and other ranges to vertically down, due to the flipping of the beam spin at certain depolarizing resonances. As described in Ref. [2], the ratios of polarizations were consistent with being constant, with magnitudes

$$P_{0+}:P_-:P_+:P_{0-}=0.072:1.000:1.000:0.072. \tag{2}$$

These four magnitudes were then multiplied by a different constant at different times as the ion source polarization changed or the accelerator depolarization varied. These conclusions are partly based on special measurements made subsequent to the experiments described in this paper; see Ref. [13]. The typical size of the beam near the polarized target was measured to be ~20 mm in diameter, and the typical magnitude of the beam polarization, P_+ or P_-, was 0.6–0.9.

Three relative beam polarimeters were used to monitor the vertical (N-type) and horizontal (S-type) transverse components of the beam polarization. These were the SD3 polarimeter [2,8] located some distance after the extraction of the beam from Saturne, the target region or antipolarimeter [2] situated slightly upstream of the polarized target, and the downstream or ''Gatchina'' polarimeter [3], that was first installed but only partially operational in run period II. They measured the vertical, horizontal, and vertical components of the beam polarization, respectively.

The polarized proton target used for these measurements is described in Refs. [2,9,10]. Details of the target material and size are given in Ref. [2]. The target operated in the frozen spin mode at a temperature as low as 40 mK and a small magnetic holding field of 0.33 T. Data with both signs of polarization were collected at each energy. The target polarization measurements were made with an NMR system, and usually occurred before entering and after leaving the frozen spin mode of operation. Initial values of the target polarization magnitude, before entering the frozen spin mode, were 0.65−0.85. The absolute target polarization was found by a comparison of the NMR signals in the polarized state and when the target material was in thermal equilibrium near 1 K. The thermal equilibrium calibrations were typically performed before and after each run period, and these calibrations agreed with each other within statistical errors.

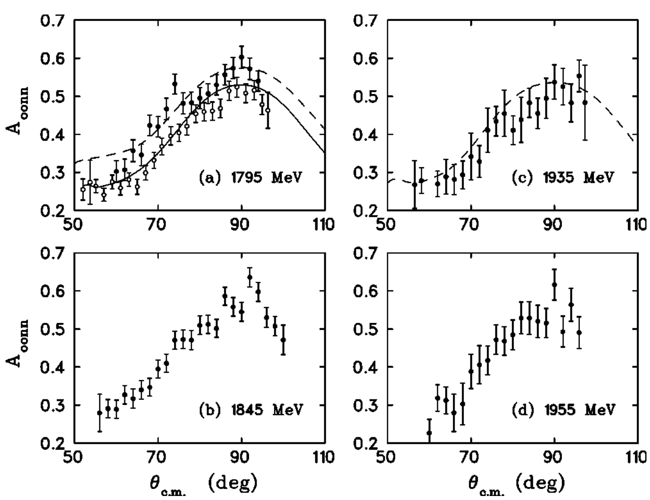

FIG. 1. Experimental results for $A_{00nn}=C_{NN}$ as a function of c.m. angle at 1795, 1845, 1935, and 1955 MeV. The closed circles are from this paper, and the open circles from Lehar *et al.* [16]. The solid curve is a PSA prediction of the Saclay-Geneva group [18], and the dashed curves are from Arndt *et al.* [19].

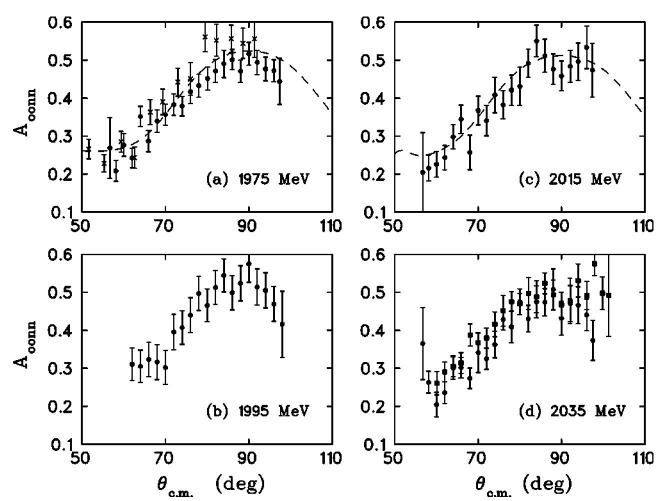

FIG. 2. Experimental results for $A_{00nn}=C_{NN}$ as a function of c.m. angle at 1975, 1995, 2015, and 2035 MeV. The values at 2035 MeV from run period I are shown as solid circles, and from run period II as solid squares. All other data from this paper are given as solid circles. The crosses are data from Bell *et al.* [15], and the dashed curves are from PSA predictions of Arndt *et al.* [19].

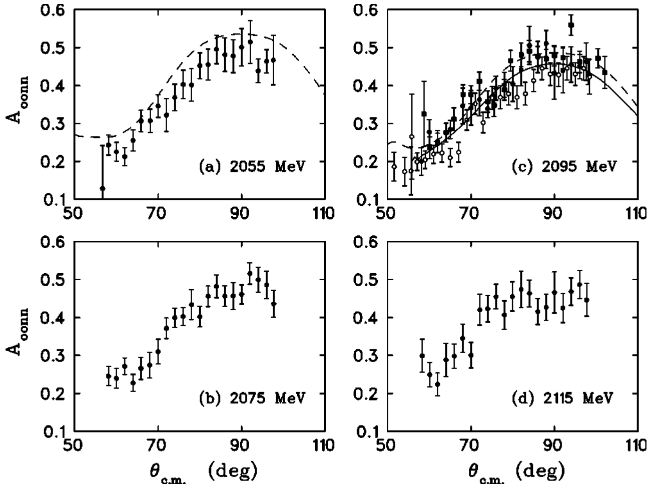

FIG. 3. Experimental results for $A_{00nn}=C_{NN}$ as a function of c.m. angle at 2055, 2075, 2095, and 2115 MeV. The values at 2095 MeV from run period I are shown as solid circles, and from run period II as solid squares. All other data from this paper are given as solid circles. The open circles are from Lehar *et al.* [16]. The solid curve is from a PSA prediction of the Saclay-Geneva group [18], and the dashed curves are from Arndt *et al.* [19].

III. EXPERIMENTAL DETECTORS

The apparatus to detect the outgoing particles was designed for *pp*, *np*, and *pn* elastic scattering measurements over a large angular range. The scattered and recoil protons in this experiment were detected in coincidence. The set of beam-right detectors consisted of a magnetic spectrometer, with trigger scintillation counters, four multiwire proportional chambers of three to four sense wire planes each (X,Y,U or X,Y,U,V), and a scintillation counter hodoscope. Its acceptance was approximately 70 msr, and the magnetic field integral was 0.74 T m. Following the hodoscope was an array of neutron counters with associated charged particle veto counters. The set of beam-left detectors included trigger scintillation counters, two multiwire proportional chambers with three sense planes each, a scintillation counter hodoscope, plus other chambers used simultaneously for measuring the polarization of these protons (not used for the A_{00nn} data).

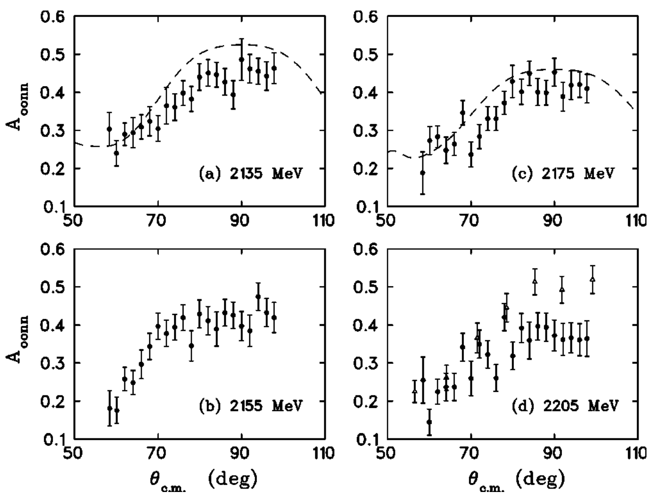

FIG. 4. Experimental results for $A_{00nn}=C_{NN}$ as a function of c.m. angle at 2135, 2155, 2175, and 2205 MeV. The closed circles are from this paper, and the open triangles from Miller *et al.* [14]. The dashed curves are from PSA predictions of Arndt *et al.* [19].

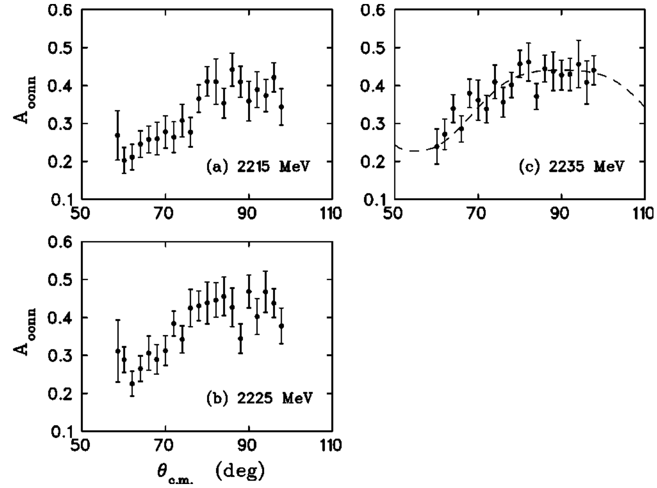

FIG. 5. Experimental results for $A_{00nn}=C_{NN}$ as a function of c.m. angle at 2215, 2225, and 2235 MeV. The closed circles are from this paper, and the dashed curve is from a PSA prediction of Arndt *et al.* [19].

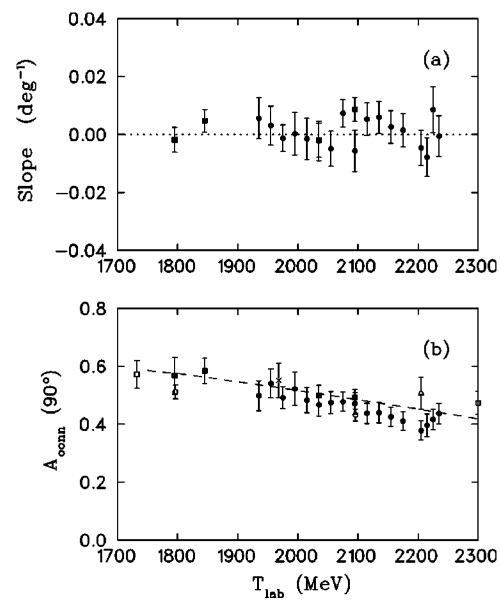

FIG. 6. Values of (a) the slope $dA_{00nn}/d\theta$ and (b) $A_{00nn}=C_{NN}$ at 90° c.m. as a function of laboratory kinetic energy. The errors shown are combined statistical and systematic uncertainties. The closed circles (run period I) and squares (run period II) are from this paper, the open triangle from Ref. [14], the cross from Ref. [15], the open circles from Ref. [16], and the open squares from Ref. [17]. The dashed curve is from a PSA prediction of Arndt *et al.* [19].

The trigger required signals in coincidence from a left and a right trigger counter, and from a left and right hodoscope counter; no information from the wire chambers was included. In addition, one or two adjacent neutron counters (used to detect protons) were required to have a signal. Information from the multiwire proportional chambers, various analog-to-digital converters and time-to-digital converters, and scalers were then read out and written to magnetic tape. Many additional details about the apparatus are given in Refs. [2,7,11,12]

IV. DATA ANALYSIS

Details of the data analysis are presented in Refs. [2,7,11]. The data analysis occurred semi-independently in two locations. Much of the off-line software was in common, but there were some important differences in cuts and other details. The results of the two analyses for A_{00nn} were in quite good agreement. The present data are also in fairly good agreement with our preliminary results from the first running period [6]. Those results are now superceded by the final data listed in the present paper.

There were several steps in the data analysis. The first step analyzed the scalar values read at the end of each spill. Spills with bad or unusual experimental conditions, or with scalar hardware problems were identified and removed with cuts. Various scalar ratios and asymmetries were computed from the polarimeter scalar data, and the information used in the evaluation of some of the elastic scattering results when sizable time dependent changes were observed.

The next step dealt with the elastic scattering events. The data were examined for changes in the relative efficiency of the hodoscope counters, wire chambers, or neutron counters as a function of time or beam polarization state. If such changes were found, the counter, wire, or wire chamber plane information was subsequently eliminated for all runs, beam, and target polarization states for that data set in order to prevent certain systematic errors.

After the cuts described above were made, the remaining elastic scattering candidate events were analyzed. The scintillation counter hodoscope, neutron counter, and multiwire proportional chamber data were decoded to give the positions of the particle tracks. Events were rejected if more than one counter was triggered in either hodoscope, or if the wire chamber data were inconsistent or insufficient to fully reconstruct the particle trajectory. Cuts were applied to the reconstructed interaction point, the observed momentum as a function of scattering angle, and the observed scattering angles of the two outgoing particles. The location of typical cuts and further details are given in Ref. [2].

After all cuts, the coplanarity of the remaining events was then computed as $\delta\phi=\phi_L+\phi_R-180°$, where ϕ_L and ϕ_R are the left and right azimuthal angles of the detected particles. The coplanarity distributions contained a peak on a small, slowly varying, and approximately symmetric background. Then the number of elastic events in the peak, after background subtraction, was estimated for each c.m. angle, and each of the target and beam polarization states. These counts were normalized to the relative, integrated beam intensity for those states. The relative intensity was obtained from the target-region polarimeter rates in the up and down arms; these rates were insensitive to the vertical component of the beam polarization.

The normalized number of elastic events for the two target polarization states and the two, three, or four beam polarization states were used to derive the values of A_N and $A_{00nn}=C_{NN}=A_{NN}$ at each c.m. angle, as well as the beam polarization magnitude, as described in Ref. [2]. The relative magnitudes of the beam polarization states were assumed to obey Eq. (2). It was also assumed that there was only a slow variation in detector efficiencies over the period of beam polarization changes (seconds), but the equations allow for drifts in efficiencies with target polarization reversals (hours).

V. RESULTS

The $A_{00nn}=C_{NN}=A_{NN}$ results at each c.m. angle are given in Table I and Figs. 1–5. Two independent analyses were performed, with slightly different cuts and other details, and the results were combined for this paper. Also, it can be seen in Figs. 2 and 3 that there is good agreement of the two data sets at 2035 and 2095 MeV, which were taken in different run periods. The quoted statistical uncertainties, ΔA_{00nn}, contain a contribution which is half the difference between the values from the two analyses. Relative errors σ_{rel} are also shown in Table I. These consist of an estimated uncertainty in the absolute target polarization ($\pm 3.0\%$) and in the value of the beam polarization used. The quantity $(1+\sigma_{rel})$ represents a multiplicative factor that moves all points of one data set up or down together. Such a normalization is usually performed for comparison of two different sets of data, for example in a phase shift analysis (PSA). Assuming a Gaussian distribution of errors, then the total uncertainty on A_{00nn} is given by

$$(\delta A_{00nn})^2=(\Delta A_{00nn})^2+(A_{00nn}\times\sigma_{rel})^2. \tag{3}$$

The A_{00nn} angular dependence for pp elastic scattering is a symmetric function with respect to 90° c.m. due to the Pauli principle [1]. Thus the value of the slope, $dA_{00nn}/d\theta$ at 90° c.m. should be zero, and this fact was used as a test on the data. The measured values for $\theta_{\text{c.m.}}=90°\pm5°$ were fit-with a straight line to yield $A_{00nn}(90°)$ as well as the slope, and these are presented in Table II and Fig. 6. The slope is seen to be consistent with zero, as expected. Based on the analyzing power measurements obtained from these same data, it appears there was probably a slight misalignment of the apparatus compared to the actual average beam direction; see Refs. [2,3]. Such a misalignment is expected to have negligible effects on the A_{00nn} results compared to the quoted statistical uncertainties.

Previous results near the energies and angles of this experiment are also shown in Figs. 1–4. These data are from the Argonne ZGS [14,15] and from Saturne [16]. The ZGS results of Bell *et al.* [15] at 1968 MeV and of Miller *et al.* [14] at 2205 MeV are both higher than the present data, while the Saturne data of Lehar *et al.* [16] at 1796 and 2096 MeV are lower in magnitude. However, only statistical errors

TABLE I. Measured values of A_{00nn} and the associated statistical errors, ΔA_{00nn}. The quantities $\langle \theta_{\mathrm{c.m.}} \rangle$ and $-t$ are the central values of the c.m. angle and four-momentum transfer squared for each bin in degrees and $(\mathrm{GeV}/c)^2$, respectively. The fractional uncertainty due to knowledge of the absolute beam and target polarization is denoted σ_{rel}.

$\langle \theta_{\mathrm{c.m.}} \rangle$	$-t$	A_{00nn}	ΔA_{00nn}
	(a) 1795 MeV, $\sigma_{rel} = \pm 0.110$		
60.0	0.842	0.302	0.028
62.0	0.894	0.307	0.029
64.0	0.946	0.357	0.029
66.0	0.999	0.346	0.028
68.0	1.053	0.424	0.027
70.0	1.108	0.420	0.027
72.0	1.164	0.466	0.028
74.0	1.220	0.532	0.026
76.0	1.277	0.481	0.028
78.0	1.334	0.483	0.028
80.0	1.392	0.495	0.028
82.0	1.450	0.507	0.026
84.0	1.508	0.530	0.027
86.0	1.567	0.557	0.027
88.0	1.625	0.574	0.028
90.0	1.684	0.602	0.029
92.0	1.743	0.572	0.028
94.0	1.802	0.540	0.027
	(b) 1845 MeV, $\sigma_{rel} = \pm 0.073$		
56.0	0.763	0.279	0.049
58.0	0.814	0.291	0.024
60.0	0.866	0.289	0.024
62.0	0.918	0.327	0.024
64.0	0.972	0.317	0.025
66.0	1.027	0.340	0.024
68.0	1.083	0.346	0.023
70.0	1.139	0.395	0.024
72.0	1.196	0.410	0.024
74.0	1.254	0.470	0.023
76.0	1.312	0.472	0.024
78.0	1.371	0.471	0.025
80.0	1.431	0.509	0.025
82.0	1.490	0.512	0.024
84.0	1.550	0.502	0.024
86.0	1.610	0.586	0.024
88.0	1.671	0.558	0.025
90.0	1.731	0.545	0.025
92.0	1.792	0.636	0.026
94.0	1.852	0.597	0.025
96.0	1.912	0.530	0.026
98.0	1.972	0.507	0.025
100.0	2.032	0.471	0.039
	(c) 1935 MeV, $\sigma_{rel} = \pm 0.095$		
56.5	0.815	0.268	0.063
58.1	0.856	0.278	0.034
59.9	0.906	0.183	0.038
62.0	0.964	0.270	0.034
64.0	1.019	0.288	0.046
66.0	1.077	0.281	0.040
	(c) 1935 MeV, $\sigma_{rel} = \pm 0.095$		
68.0	1.136	0.293	0.037
70.0	1.194	0.342	0.061
72.0	1.254	0.329	0.041
74.0	1.315	0.411	0.058
76.0	1.377	0.434	0.039
78.0	1.437	0.455	0.061
80.1	1.502	0.410	0.038
82.0	1.563	0.438	0.059
84.0	1.627	0.482	0.038
86.0	1.688	0.455	0.040
88.0	1.751	0.494	0.053
90.0	1.815	0.537	0.045
92.0	1.880	0.525	0.048
94.0	1.942	0.483	0.050
95.9	2.003	0.553	0.041
97.3	2.047	0.483	0.098
	(d) 1955 MeV, $\sigma_{rel} = \pm 0.086$		
60.0	0.916	0.226	0.036
62.0	0.973	0.318	0.035
64.0	1.030	0.312	0.035
65.9	1.087	0.280	0.049
68.0	1.148	0.303	0.055
70.0	1.207	0.388	0.045
72.0	1.267	0.406	0.050
74.0	1.329	0.417	0.038
76.0	1.391	0.472	0.039
78.0	1.453	0.468	0.038
80.0	1.517	0.484	0.039
82.0	1.580	0.529	0.042
84.0	1.643	0.528	0.043
86.0	1.706	0.520	0.043
88.0	1.770	0.515	0.039
90.0	1.834	0.616	0.040
92.0	1.900	0.493	0.040
94.0	1.962	0.563	0.043
95.9	2.024	0.490	0.042
	(e) 1975 MeV, $\sigma_{rel} = \pm 0.072$		
56.7	0.836	0.268	0.080
58.1	0.874	0.208	0.028
60.0	0.925	0.276	0.030
62.0	0.983	0.242	0.026
64.0	1.041	0.352	0.027
65.9	1.098	0.286	0.028
68.0	1.160	0.339	0.029
70.0	1.219	0.356	0.028
72.0	1.281	0.383	0.028
74.0	1.342	0.379	0.026
76.0	1.405	0.417	0.031
78.0	1.468	0.432	0.030

TABLE I. (*Continued*).

$\langle \theta_{c.m.} \rangle$	$-t$	A_{00nn}	ΔA_{00nn}
	(e) 1975 MeV, $\sigma_{rel} = \pm 0.072$		
80.1	1.533	0.451	0.030
82.0	1.595	0.471	0.030
84.0	1.660	0.490	0.036
86.0	1.723	0.501	0.027
88.0	1.788	0.470	0.029
90.0	1.853	0.516	0.030
92.0	1.919	0.494	0.032
94.0	1.983	0.477	0.031
96.0	2.046	0.472	0.029
97.4	2.092	0.444	0.061
	(f) 1995 MeV, $\sigma_{rel} = \pm 0.101$		
62.0	0.993	0.311	0.043
64.0	1.051	0.305	0.043
66.0	1.111	0.323	0.045
68.0	1.171	0.316	0.046
70.0	1.232	0.302	0.045
72.0	1.293	0.395	0.047
74.0	1.356	0.407	0.044
76.0	1.419	0.440	0.046
78.0	1.483	0.497	0.045
80.0	1.547	0.466	0.043
82.0	1.611	0.513	0.044
84.0	1.676	0.544	0.044
86.0	1.741	0.499	0.045
88.0	1.807	0.524	0.047
90.0	1.872	0.575	0.049
92.0	1.937	0.514	0.048
94.0	2.002	0.505	0.046
96.0	2.068	0.469	0.046
98.0	2.132	0.416	0.087
	(g) 2015 MeV, $\sigma_{rel} = \pm 0.079$		
56.7	0.853	0.204	0.105
58.1	0.891	0.216	0.034
60.0	0.946	0.226	0.034
62.0	1.003	0.243	0.032
64.0	1.062	0.298	0.032
65.9	1.120	0.344	0.037
68.0	1.184	0.257	0.045
70.0	1.243	0.367	0.038
72.0	1.307	0.340	0.040
74.0	1.369	0.408	0.047
76.0	1.434	0.382	0.037
78.0	1.497	0.421	0.040
80.0	1.564	0.431	0.050
82.0	1.627	0.492	0.037
84.0	1.693	0.550	0.042
86.0	1.758	0.512	0.044
88.0	1.824	0.476	0.040
90.0	1.890	0.458	0.039
92.1	1.960	0.483	0.043

$\langle \theta_{c.m.} \rangle$	$-t$	A_{00nn}	ΔA_{00nn}
	(g) 2015 MeV, $\sigma_{rel} = \pm 0.079$		
94.0	2.022	0.496	0.049
96.0	2.088	0.534	0.056
97.4	2.136	0.474	0.071
	(h) 2035 MeV (I), $\sigma_{rel} = \pm 0.070$		
56.7	0.862	0.365	0.095
58.1	0.900	0.263	0.029
60.0	0.955	0.204	0.032
62.0	1.013	0.235	0.028
64.0	1.072	0.300	0.029
65.9	1.130	0.302	0.027
68.0	1.194	0.273	0.027
70.0	1.256	0.342	0.053
72.0	1.319	0.325	0.028
74.0	1.383	0.362	0.035
76.0	1.447	0.428	0.027
78.0	1.512	0.409	0.042
80.0	1.578	0.475	0.034
82.0	1.644	0.430	0.035
84.0	1.710	0.475	0.042
86.0	1.776	0.474	0.036
88.0	1.843	0.507	0.054
90.0	1.909	0.431	0.044
92.1	1.979	0.470	0.048
94.0	2.042	0.466	0.049
96.0	2.109	0.440	0.042
97.5	2.159	0.374	0.053
	(i) 2035 MeV (II), $\sigma_{rel} = \pm 0.064$		
60.1	0.959	0.261	0.031
62.0	1.013	0.290	0.026
64.0	1.072	0.305	0.028
65.9	1.130	0.314	0.027
68.1	1.197	0.387	0.029
70.0	1.256	0.367	0.025
72.0	1.319	0.379	0.026
74.0	1.383	0.416	0.033
76.0	1.447	0.451	0.041
78.0	1.512	0.475	0.026
80.0	1.578	0.469	0.028
82.1	1.647	0.497	0.042
84.0	1.710	0.488	0.042
86.0	1.776	0.523	0.028
88.0	1.843	0.493	0.039
90.0	1.909	0.467	0.033
92.0	1.976	0.477	0.060
94.0	2.042	0.531	0.044
96.0	2.109	0.492	0.037
97.9	2.173	0.575	0.031
99.8	2.234	0.498	0.043
101.3	2.283	0.492	0.108

TABLE I. (*Continued*).

$\langle \theta_{c.m.} \rangle$	$-t$	A_{00nn}	ΔA_{00nn}
(j) 2055 MeV, $\sigma_{rel}=\pm 0.070$			
56.7	0.871	0.128	0.113
58.1	0.908	0.243	0.026
60.0	0.965	0.225	0.025
62.0	1.023	0.212	0.024
64.0	1.083	0.255	0.028
65.9	1.141	0.306	0.028
68.1	1.208	0.307	0.031
70.0	1.268	0.346	0.030
72.0	1.334	0.322	0.044
74.0	1.397	0.368	0.035
76.0	1.462	0.403	0.038
78.0	1.527	0.401	0.043
80.0	1.594	0.452	0.034
82.0	1.659	0.455	0.041
84.0	1.726	0.495	0.038
86.0	1.793	0.481	0.044
88.0	1.861	0.477	0.044
90.0	1.928	0.501	0.049
92.1	1.997	0.514	0.056
94.0	2.063	0.439	0.031
96.0	2.129	0.464	0.031
97.6	2.183	0.467	0.065
(k) 2075 MeV, $\sigma_{rel}=\pm 0.064$			
58.1	0.919	0.246	0.025
60.0	0.974	0.240	0.026
62.0	1.033	0.271	0.022
64.0	1.093	0.227	0.023
65.9	1.153	0.266	0.029
68.0	1.219	0.274	0.034
70.0	1.280	0.310	0.033
72.0	1.347	0.371	0.027
74.0	1.409	0.399	0.025
76.0	1.476	0.403	0.024
78.0	1.543	0.434	0.039
80.0	1.608	0.402	0.027
82.0	1.676	0.456	0.027
84.0	1.743	0.482	0.030
86.0	1.811	0.456	0.027
88.0	1.879	0.457	0.036
90.0	1.946	0.461	0.025
92.0	2.016	0.516	0.029
94.0	2.082	0.499	0.033
96.0	2.151	0.486	0.036
97.7	2.207	0.436	0.035
(l) 2095 MeV (I), $\sigma_{rel}=\pm 0.068$			
58.1	0.928	0.200	0.036
60.0	0.984	0.277	0.033
62.0	1.043	0.252	0.029
65.0	1.135	0.284	0.024
68.0	1.231	0.346	0.047
70.0	1.293	0.341	0.046
(l) 2095 MeV (I), $\sigma_{rel}=\pm 0.068$			
72.0	1.358	0.363	0.043
74.0	1.424	0.339	0.024
76.0	1.490	0.393	0.032
78.0	1.557	0.402	0.033
80.0	1.624	0.404	0.046
82.0	1.692	0.441	0.042
84.0	1.760	0.505	0.050
86.0	1.829	0.475	0.041
88.0	1.897	0.510	0.035
90.0	1.966	0.433	0.069
92.0	2.034	0.440	0.059
94.0	2.103	0.455	0.047
96.0	2.171	0.450	0.032
97.6	2.227	0.463	0.050
(m) 2095 MeV (II), $\sigma_{rel}=\pm 0.050$			
58.7	0.945	0.325	0.086
60.1	0.985	0.236	0.029
62.0	1.043	0.248	0.026
64.0	1.104	0.276	0.025
65.9	1.164	0.311	0.030
68.1	1.232	0.376	0.026
70.0	1.293	0.376	0.024
72.0	1.358	0.411	0.024
74.0	1.424	0.357	0.028
75.5	1.473	0.347	0.029
78.0	1.557	0.388	0.027
79.5	1.607	0.465	0.027
82.0	1.692	0.480	0.031
84.0	1.760	0.490	0.028
86.0	1.829	0.476	0.026
88.0	1.897	0.470	0.025
90.0	1.966	0.478	0.027
92.0	2.034	0.473	0.029
94.0	2.103	0.559	0.027
96.0	2.171	0.462	0.029
98.0	2.239	0.431	0.029
100.4	2.322	0.472	0.025
102.0	2.374	0.434	0.042
(n) 2115 MeV, $\sigma_{rel}=\pm 0.071$			
58.3	0.942	0.299	0.043
60.1	0.995	0.249	0.032
62.0	1.052	0.224	0.030
64.0	1.115	0.288	0.044
66.0	1.176	0.298	0.032
68.0	1.243	0.345	0.037
70.0	1.306	0.300	0.034
72.1	1.374	0.420	0.041
74.0	1.437	0.423	0.035
76.0	1.504	0.455	0.032
78.0	1.572	0.406	0.037

TABLE I. (*Continued*).

$\langle\theta_{c.m.}\rangle$	$-t$	A_{00nn}	ΔA_{00nn}
	(n) 2115 MeV, $\sigma_{rel}=\pm 0.071$		
79.9	1.636	0.455	0.039
82.0	1.709	0.474	0.048
84.0	1.777	0.463	0.035
86.0	1.847	0.416	0.034
88.0	1.914	0.427	0.035
90.0	1.983	0.466	0.054
92.0	2.054	0.425	0.039
94.0	2.123	0.468	0.036
96.0	2.192	0.487	0.037
97.7	2.251	0.446	0.043
	(o) 2135 MeV, $\sigma_{rel}=\pm 0.070$		
58.3	0.952	0.303	0.044
60.0	1.003	0.240	0.033
62.0	1.062	0.290	0.030
64.0	1.125	0.294	0.039
66.0	1.188	0.309	0.032
68.0	1.254	0.324	0.038
70.0	1.318	0.305	0.034
72.0	1.385	0.365	0.048
74.0	1.451	0.361	0.035
76.0	1.519	0.398	0.033
78.0	1.587	0.382	0.033
79.9	1.654	0.440	0.035
82.0	1.725	0.451	0.035
84.0	1.794	0.446	0.033
86.0	1.864	0.427	0.035
88.0	1.932	0.393	0.037
90.0	2.002	0.486	0.054
92.0	2.073	0.462	0.037
94.0	2.143	0.455	0.034
96.0	2.213	0.443	0.037
97.8	2.274	0.463	0.041
	(p) 2155 MeV, $\sigma_{rel}=\pm 0.067$		
58.4	0.962	0.181	0.047
60.1	1.013	0.176	0.035
62.0	1.073	0.258	0.031
64.0	1.136	0.249	0.032
66.0	1.199	0.296	0.038
68.0	1.265	0.344	0.035
70.0	1.330	0.396	0.035
72.0	1.397	0.378	0.034
74.0	1.465	0.394	0.034
76.0	1.533	0.419	0.034
78.0	1.602	0.345	0.040
79.9	1.668	0.429	0.036
82.0	1.742	0.411	0.037
84.0	1.810	0.389	0.045
86.0	1.881	0.432	0.035
88.0	1.951	0.425	0.035

$\langle\theta_{c.m.}\rangle$	$-t$	A_{00nn}	ΔA_{00nn}
	(p) 2155 MeV, $\sigma_{rel}=\pm 0.067$		
90.0	2.021	0.397	0.038
92.0	2.092	0.384	0.041
94.0	2.163	0.474	0.036
96.0	2.233	0.432	0.037
97.8	2.295	0.419	0.040
	(q) 2175 MeV, $\sigma_{rel}=\pm 0.067$		
58.4	0.972	0.188	0.056
60.1	1.022	0.273	0.037
62.0	1.083	0.283	0.028
64.0	1.146	0.248	0.034
66.0	1.211	0.264	0.030
68.0	1.276	0.346	0.032
70.0	1.343	0.237	0.033
72.0	1.410	0.284	0.032
74.0	1.479	0.331	0.032
76.0	1.547	0.330	0.031
78.0	1.616	0.372	0.030
79.9	1.684	0.428	0.042
82.1	1.759	0.401	0.033
84.0	1.827	0.450	0.032
86.0	1.899	0.400	0.035
88.0	1.968	0.399	0.033
90.0	2.041	0.453	0.037
92.0	2.111	0.388	0.038
94.0	2.183	0.418	0.037
96.0	2.254	0.420	0.034
97.8	2.317	0.410	0.038
	(r) 2205 MeV, $\sigma_{rel}=\pm 0.073$		
58.5	0.988	0.255	0.061
60.0	1.036	0.145	0.034
62.0	1.098	0.225	0.033
64.0	1.162	0.237	0.036
66.0	1.228	0.237	0.036
68.0	1.293	0.342	0.037
70.0	1.360	0.259	0.046
72.0	1.431	0.349	0.037
74.0	1.500	0.322	0.036
76.0	1.568	0.260	0.035
78.0	1.639	0.420	0.036
80.0	1.709	0.318	0.036
82.1	1.783	0.392	0.038
84.0	1.852	0.359	0.048
86.0	1.925	0.396	0.036
88.0	1.996	0.394	0.037
90.0	2.069	0.372	0.041
92.0	2.140	0.362	0.042
94.0	2.214	0.366	0.039
96.0	2.285	0.361	0.042
97.8	2.349	0.364	0.047

TABLE I. (*Continued*).

$\langle\theta_{c.m.}\rangle$	$-t$	A_{00nn}	ΔA_{00nn}
	(s) 2215 MeV, $\sigma_{rel}=\pm 0.085$		
58.5	0.994	0.268	0.065
60.1	1.041	0.202	0.034
62.0	1.103	0.211	0.034
64.0	1.167	0.245	0.035
66.0	1.233	0.258	0.035
68.0	1.299	0.260	0.043
70.0	1.367	0.278	0.042
72.0	1.436	0.264	0.040
74.0	1.505	0.307	0.043
76.0	1.575	0.277	0.039
78.0	1.646	0.365	0.036
80.0	1.717	0.410	0.039
82.1	1.793	0.410	0.060
84.0	1.861	0.353	0.039
86.0	1.934	0.442	0.043
88.0	2.006	0.409	0.041
90.0	2.078	0.359	0.052
92.0	2.150	0.389	0.047
94.1	2.226	0.373	0.043
96.0	2.296	0.421	0.039
97.8	2.359	0.344	0.048
	(t) 2225 MeV, $\sigma_{rel}=\pm 0.070$		
58.6	1.000	0.311	0.082
60.1	1.046	0.289	0.034
62.0	1.108	0.225	0.033
64.0	1.172	0.265	0.034
66.0	1.239	0.306	0.045
67.9	1.303	0.290	0.039
70.0	1.374	0.312	0.039
72.0	1.444	0.384	0.033
74.0	1.512	0.342	0.036
76.0	1.583	0.425	0.049
	(t) 2225 MeV, $\sigma_{rel}=\pm 0.070$		
78.0	1.654	0.430	0.040
80.0	1.725	0.438	0.055
82.1	1.800	0.446	0.046
84.0	1.869	0.456	0.051
86.0	1.942	0.426	0.051
88.0	2.014	0.344	0.039
90.0	2.088	0.468	0.043
92.0	2.160	0.402	0.048
94.0	2.233	0.468	0.054
96.0	2.306	0.438	0.038
97.8	2.370	0.378	0.047
	(u) 2235 MeV, $\sigma_{rel}=\pm 0.066$		
60.1	1.050	0.239	0.046
62.0	1.113	0.272	0.040
64.0	1.178	0.339	0.037
66.0	1.244	0.286	0.035
67.9	1.310	0.379	0.038
70.0	1.380	0.361	0.053
72.0	1.449	0.338	0.036
74.0	1.520	0.409	0.045
76.0	1.590	0.356	0.039
78.0	1.661	0.401	0.034
80.0	1.733	0.457	0.036
82.1	1.809	0.462	0.050
84.0	1.878	0.371	0.034
86.0	1.951	0.444	0.035
88.0	2.024	0.437	0.051
90.0	2.097	0.428	0.039
92.0	2.169	0.429	0.043
94.1	2.246	0.456	0.063
96.0	2.316	0.408	0.057
97.7	2.380	0.440	0.039

are shown in the figures. When the normalization factors, corresponding to the systematic absolute beam and target polarization uncertainties, are included, the agreement is quite acceptable.

Data from Lin *et al.* [17] from the Argonne ZGS and also from Refs. [14–16] are plotted in Fig. 6. Both statistical and quoted systematic uncertainties are included in the errors shown. Excellent agreement is seen with the present results.

Recently, the Saclay-Geneva group performed a direct reconstruction of the pp elastic scattering amplitudes and a phase shift analysis (Ref. [18]) at four fixed, high energies where complete sets of spin observables had been measured, namely at 1800, 2100, 2400, and 2700 MeV. The predictions for A_{00nn} are shown at 1795 and 2095 MeV in Figs. 1 and 3. Also, the Arndt *et al.* energy-dependent PSA was recently extended from 1.6 to 2.5 GeV [19]. Their predictions using the SAID solution SP99 at selected energies are given in Figs. 1–5. Note that energy-dependent PSAs describe the angular dependence of all observables over a large energy interval, and may average over possible local energy variations. Nevertheless, the PSA predictions reproduce the data reasonably well and agree closely at both 1795 and 2095 MeV. The data from Refs. [2,3] and this paper are included in the recent data bases of both Arndt *et al.* and the Saclay-Geneva group, but the results from this paper are not in the data base for the Arndt *et al.* SP99 solution. However, the good agreement of the PSA predictions and the present results is not surprising, since the new data are consistent with previous measurements and since the PSAs are anchored by the complete sets of spin observables at the four energies noted above.

The data from run periods I and II, shown in Figs. 1–5, will make a major contribution to the pp elastic scattering data base. A total of 21 data sets, at 19 beam kinetic energies, and 442 different points, are included. There is satisfactory agreement with previous measurements, and between data from run periods I and II when measure-

TABLE II. Results from straight line fits to the A_{00nn} data near 90° c.m. The beam kinetic energy, fitted slope, and value at 90° are presented. The 90° data include systematic errors. The value of χ^2 per degree of freedom for the weighted average is 0.72.

Energy (MeV)	Slope ($\deg^{-1}$)	$A_{00nn}(90°)$
1795	-0.0018 ± 0.0043	0.568 ± 0.064
1845	0.0047 ± 0.0039	0.584 ± 0.044
1935	0.0056 ± 0.0071	0.498 ± 0.052
1955	0.0031 ± 0.0067	0.541 ± 0.050
1975	-0.0013 ± 0.0046	0.492 ± 0.038
1995	0.0003 ± 0.0073	0.522 ± 0.057
2015	-0.0015 ± 0.0071	0.483 ± 0.043
2035I	-0.0022 ± 0.0068	0.466 ± 0.038
2035II	-0.0020 ± 0.0059	0.499 ± 0.036
2055	-0.0049 ± 0.0061	0.474 ± 0.038
2075	0.0073 ± 0.0047	0.478 ± 0.033
2095I	-0.0057 ± 0.0071	0.472 ± 0.038
2095II	0.0087 ± 0.0042	0.493 ± 0.027
2115	0.0053 ± 0.0056	0.438 ± 0.035
2135	0.0059 ± 0.0055	0.440 ± 0.035
2155	0.0026 ± 0.0057	0.426 ± 0.033
2175	0.0015 ± 0.0057	0.411 ± 0.032
2205	-0.0046 ± 0.0060	0.378 ± 0.033
2215	-0.0078 ± 0.0067	0.397 ± 0.039
2225	0.0086 ± 0.0079	0.416 ± 0.036
2235	-0.0006 ± 0.0071	0.437 ± 0.035
Wt. av.	0.0016 ± 0.0012	

ments were repeated at the same beam energy. Many of the data sets are at energies and angles where no previous A_{00nn} results exist.

ACKNOWLEDGMENTS

We wish to express our gratitude to all the operations staff of the Saturne II accelerator for excellent performance of the polarized beams. We are also indebted to C. Lechanoine-LeLuc, E. Lomon, and J. Comfort for their encouraging suggestions. This work was supported in part by the U.S. Department of Energy, Division of Nuclear Physics, Contract No. W-31-109-ENG-38, by the Swiss National Science Foundation, and by the Russian Foundation for Fundamental Physics Program 122.03.

[1] J. Bystricky, F. Lehar, and P. Winternitz, J. Phys. (Paris) **39**, 1 (1978).

[2] C. E. Allgower, J. Ball, L. S. Barabash, P.-Y. Beauvais, M. E. Beddo, Y. Bedfer, N. Borisov, A. Boutefnouchet, J. Bystrický, P. A. Chamouard, M. Combet, Ph. Demierre, J.-M. Fontaine, V. Ghazikhanian, D. P. Grosnick, R. Hess, Z. Janout, Z. F. Janout, V. A. Kalinnikov, T. E. Kasprzyk, Yu. M. Kazarinov, B. A. Khachaturov, R. Kunne, J. M. Lagniel, F. Lehar, J. L. Lemaire, A. de Lesquen, D. Lopiano, M. de Mali, V. N. Matafonov, G. Milleret, I. L. Pisarev, A. A. Popov, A. N. Prokofiev, D. Rapin, J. L. Sans, H. M. Spinka, Yu. A. Usov, V. V. Vikhrov, B. Vuaridel, C. A. Whitten, and A. A. Zhdanov, Phys. Rev. C **60**, 054001 (1999).

[3] C. E. Allgower, J. Ball, M. E. Beddo, J. Bystrický, P.-A. Chamouard, M. Combet, Ph. Demierre, J.-M. Fontaine, D. P. Grosnick, R. Hess, Z. Janout, Z. F. Janout, V. A. Kalinnikov, T. E. Kasprzyk, B. A. Khachaturov, R. Kunne, F. Lehar, A. de Lesquen, D. Lopiano, M. de Mali, V. N. Matafonov, I. L. Pisarev, A. A. Popov, A. N. Prokofiev, D. Rapin, J.-L. Sans, H. M. Spinka, A. Teglia, Yu. A. Usov, V. V. Vikhrov, B. Vuaridel, and A. A. Zhdanov, Phys. Rev. C **60**, 054002 (1999).

[4] C. E. Allgower, J. Ball, M. Beddo, Y. Bedfer, A. Boutefnouchet, J. Bystricky, P.-A. Chamouard, Ph. Demierre, J.-M. Fontaine, V. Ghazikhanian, D. Grosnick, R. Hess, Z. Janout, V. A. Kalinnikov, T. E. Kasprzyk, B. A. Khachaturov, R. Kunne, F. Lehar, A. de Lesquen, D. Lopiano, V. N. Matafonov, I. L. Pisarev, A. A. Popov, A. N. Prokofiev, D. Rapin, J.-L. Sans, H. M. Spinka, A. Teglia, Yu. A. Usov, V. V. Vikhrov, B. Vuaridel, C. A. Whitten, and A. A. Zhdanov, Nucl. Phys. **A637**, 231 (1998).

[5] C. E. Allgower, J. Ball, L. S. Barabash, M. Beddo, Y. Bedfer, A. Boutefnouchet, J. Bystricky, P.-A. Chamouard, Ph. Demierre, J.-M. Fontaine, V. Ghazikhanian, D. Grosnick, R. Hess, Z. Janout, Z. F. Janout, V. A. Kalinnikov, T. E. Kasprzyk, Yu. M. Kazarinov, B. A. Khachaturov, R. Kunne, C. Lechanoine-LeLuc, F. Lehar, A. de Lesquen, D. Lopiano, M. de Mali, V. N. Matafonov, I. L. Pisarev, A. A. Popov, A. N. Prokofiev, D. Rapin, J.-L. Sans, H. M. Spinka, Yu. A. Usov, V. V. Vikhrov, B. Vuaridel, C. A. Whitten, and A. A. Zhdanov, Eur. Phys. J. C **5**, 453 (1998).

[6] J. Ball, P. A. Chamouard, M. Combet, J. M. Fontaine, R. Kunne, J. M. Lagniel, J. L. Lemaire, G. Milleret, J. L. Sans, J. Bystricky, F. Lehar, A. de Lesquen, M. de Mali, Ph. Demierre, R. Hess, Z. F. Janout, E. L. Lomon, D. Rapin, B. Vuaridel, L. S. Barabash, Z. Janout, V. A. Kalinnikov, Yu. M. Kazarinov, B. A. Khachaturov, V. N. Matafonov, I. L. Pisarev, A. A. Popov, Yu. A. Usov, M. Beddo, D. Grosnick, T. Kasprzyk, D. Lopiano, H. Spinka, A. Boutefnouchet, V. Ghazikhanian, and C. A. Whitten, Phys. Lett. B **320**, 206 (1994).

[7] C. E. Allgower, Ph.D. thesis, Arizona State University; Argonne National Laboratory Report No. ANL-HEP-TR-97-71, 1997.

[8] J. Bystricky, J. Derégel, F. Lehar, A. de Lesquen, L. van Rossum, J. M. Fontaine, F. Perrot, C. A. Whitten, T. Hasegawa, C. R. Newsom, W. R. Leo, Y. Onel, S. Dalla Torre-Colautti, A. Penzo, H. Azaiez, and A. Michalowicz, Nucl. Instrum. Methods Phys. Res. A **239**, 131 (1985).

[9] R. Bernard, P. Chaumette, P. Chesny, J. Derégel, R. Duthil, J. Fabre, C. Lesmond, G. Seité, J. Ball, T. I. Niinikoski, and M. Rieubland, Nucl. Instrum. Methods Phys. Res. A **249**, 176 (1986).

[10] J. Ball, M. Combet, J.-L. Sans, B. Benda, P. Chaumette, J. Derégel, G. Durand, A. P. Dzyubak, C. Gaudron, F. Lehar, A. de Lesquen, T. E. Kasprzyk, Z. Janout, B. A. Khachaturov, V. N. Matafonov, and Yu. A. Usov, Nucl. Instrum. Methods Phys. Res. A **381**, 4 (1996).

[11] M. Arignon, J. Bystricky, J. Derégel, F. Lehar, A. de Lesquen, F. Petit, L. van Rossum, J. M. Fontaine, F. Perrot, J. Ball, and C. D. Lac, Nucl. Instrum. Methods Phys. Res. A **262**, 207 (1987).

[12] J. Ball, Ph. Chesny, M. Combet, J. M. Fontaine, R. Kunne, J. L. Sans, J. Bystricky, C. D. Lac, D. Legrand, F. Lehar, A. de Lesquen, M. de Mali, F. Perrot-Kunne, L. van Rossum, P. Bach, Ph. Demierre, G. Gaillard, R. Hess, Z. F. Janout, D. Rapin, Ph. Sormani, B. Vuaridel, J. P. Goudour, R. Binz, A. Klett, E. Rössle, H. Schmitt, L. S. Barabash, Z. Janout, V. A. Kalinnikov, Yu. M. Kazarinov, B. A. Khachaturov, V. N. Matafonov, I. L. Pisarev, A. A. Popov, Yu. A. Usov, M. Beddo, D. Grosnick, T. Kasprzyk, D. Lopiano, and H. Spinka, Nucl. Instrum. Methods Phys. Res. A **327**, 308 (1993).

[13] C. E. Allgower, J. Arvieux, P. Ausset, J. Ball, P.-Y. Beauvais, Y. Bedfer, J. Bystricky, P.-A. Chamouard, P. Demierre, J.-M. Fontaine, Z. Janout, V. A. Kalinnikov, T. E. Kasprzyk, B. A. Khachaturov, R. Kunne, J.-M. Lagniel, F. Lehar, A. de Lesquen, A. A. Popov, A. N. Prokofiev, D. Rapin, J.-L. Sans, H. M. Spinka, A. Teglia, V. V. Vikhrov, B. Vuaridel, and A. A. Zhdanov, Nucl. Instrum. Methods Phys. Res. A **399**, 171 (1997).

[14] D. Miller, C. Wilson, R. Giese, D. Hill, K. Nield, P. Rynes, B. Sandler, and A. Yokosawa, Phys. Rev. D **16**, 2016 (1977).

[15] D. A. Bell, J. A. Buchanan, M. M. Calkin, J. M. Clement, W. H. Dragoset, M. Furić, K. A. Johns, J. D. Lesikar, H. E. Miettinen, T. A. Mulera, G. S. Mutchler, G. C. Phillips, J. B. Roberts, and S. E. Turpin, Phys. Lett. **94B**, 310 (1980).

[16] F. Lehar, A. de Lesquen, J. P. Meyer, L. van Rossum, P. Chaumette, J. Derégel, J. Fabre, J. M. Fontaine, F. Perrot, J. Ball, C. D. Lac, A. Michalowicz, Y. Onel, D. Adams, J. Bystricky, V. Ghazikhanian, C. A. Whitten, and A. Penzo, Nucl. Phys. **B294**, 1013 (1987).

[17] A. Lin, J. R. O'Fallon, L. G. Ratner, P. F. Schultz, K. Abe, D. G. Crabb, R. C. Fernow, A. D. Krisch, A. J. Salthouse, B. Sandler, and K. M. Terwilliger, Phys. Lett. **74B**, 273 (1978).

[18] J. Bystrický, C. Lechanoine-LeLuc, and F. Lehar, Eur. Phys. J. C **4**, 607 (1998).

[19] R. A. Arndt, C. H. Oh, I. I. Strakovsky, R. L. Workman, and F. Dohrmann, Phys. Rev. C **56**, 3005 (1997); SAID solution SP99.